Shake Table Tests of Stochastic Optimal Polynomial Control of Two Span Bridge Equipped with MR Dampers

Omar El-Khoury
Graduate Student, Dept. of Civil, Environmental, & Geodetic Engineering, Ohio State University, Columbus, USA

Chunggil Kim
Graduate Student, Dept. of Civil Engineering, Chungnam National University, Daejeon, South Korea

Abdollah Shafieezadeh
Assistant Professor, Dept. of Civil, Environmental, & Geodetic Engineering, Ohio State University, Columbus, USA

Jee-Eun Hur
Visiting Assistant Professor, Dept. of Civil, Environmental, & Geodetic Engineering, Ohio State University, Columbus, USA

Gwang-Hee Heo
Professor, Dept. of Civil Engineering, Konyang University, Nonsan, South Korea

ABSTRACT: This paper studies a nonlinear feedback controller based on Optimal Polynomial Control (OPC) in semi-actively controlled systems. OPC, for instance, is an extension to conventional linear quadratic regulator (LQR), where the cost function is of higher order and the control force is decomposed into linear and nonlinear terms. The main challenges of this state-space based control design method are nonlinearity of the system and the selection of covariance matrices. Traditionally, linearization is based on deterministic elastic strategies and that usually does not incorporate stochasticity or nonlinearity in the system. To overcome this limitation, a stochastic linearization of the passive system is considered which replaces the nonlinear portion of the system behavior with an equivalent linear model, where stochasticity of excitation and nonlinearity of the system are both preserved. Then, global optimization is conducted on the nonlinear system to determine the optimal covariance matrices. The OPC approach combined with stochastic linearization is referred to as Stochastic OPC (SOPC). For verification, the effectiveness of this control algorithm is analyzed, and tested via shake table experiments on a two span-bridge equipped with MR damper and subjected to pounding between spans and span to abutment.

1. INTRODUCTION

Semi-active technology has been suggested by researchers to combine both properties of passive and active systems. For instance, the semi-active system is modified though physical parameters of passive systems with a small power requirement as opposed to active systems. In addition, semi-active devices are efficient for a wide range of excitations as opposed to passive devices that are effective for a limited bandwidth only. Magnetorheological (MR) dampers are one of the widely used semi-active devices in various control problems (Fan et al., 2009; Prabakar et al., 2013). However, some of the challenges in the control design of semi-active MR dampers are the highly nonlinear

dynamics of the device and constraints on achievable control forces.

In addition, another challenge encountered in uncontrolled or controlled structural systems under extreme loadings of earthquakes and other hazards is the nonlinear behavior in the system. It is commonly argued that the purpose for the application of control strategies is to reduce the structural response and limit the extent of nonlinearities so that the system remains nearly linear elastic during the hazard. However, hazards are stochastic events with characteristics that are not fully known prior to the occurrence. This complicates the design of a controller that can ensure linear system behavior or a behavior with limited nonlinearity. On the other hand, in some applications such as the one in this study, the goal of the control strategy is to reduce the likelihood of extreme responses in critical demand measures to limit the potential of extensive damage in the system, while accepting presence of nonlinear behavior in the system response. This strategy will allow for more cost-effective solutions based on structural control. However, this strategy poses a challenge considering that control algorithms are normally designed for systems with linear models.

To consider the limitations mentioned earlier, stochastic linearization is considered in order to incorporate nonlinearity of the system, dynamics of semi-active device, and stochasticity of the response and the excitation. Stochastic linearization method maintains the nonlinearity in the system components by replacing it by equivalent linear models (Basili and Angelis, 2007) as opposed to conventional and deterministic linearization that considers the linear elastic stiffness of the system. Then, for control design, a nonlinear feedback control algorithm, known as Optimal Polynomial Control (OPC) (Agrawal and Yang, 1996) is considered to determine optimal control forces of the MR damper. Fundamentally, the OPC algorithm is a generalization of the Linear Quadratic Regulator (LQR) algorithm through inclusion of higher order convex polynomials in the objective function, which provides more flexibility and better control improvement as compared to LQR algorithm. The OPC approach combined with stochastic linearization is referred to as Stochastic Optimal Polynomial Control (SOPC), to distinguish the strategy from the OPC method with initial elastic models. To optimize the gain matrices in the SOPC objective function a global search based on Genetic Algorithm (GA) and Monte-Carlo simulations of the semi-actively controlled system are used to perform a second level optimization. To present this methodology, seismic response mitigation of a multi-span bridge with nonlinear bearings using MR dampers is first analyzed and then tested via a set of shake table experiments.

2. STOCHASTIC OPTIMAL POLYNOMIAL CONTROL

Linear control algorithms, such as LQR for fully observable systems and Linear Quadratic Gaussian (LQG) for partially observable systems were proven to be useful in mitigating various responses in many active and semi-active control design applications. However, the LQR objective function has a restricted form and only contains polynomial functions of the second degree. The LQR algorithm can be extended to OPC control algorithm that incorporates higher order convex polynomials in the objective function. The higher order performance index for OPC is defined as (Agrawal and Yang, 1996).

$$J = \int_0^\infty (\mathbf{X^T Q_1 X} + \mathbf{u^T R u} + h(\mathbf{X}))\, \mathrm{d}t \quad (1)$$

where $\mathbf{X}$ and $\mathbf{u}$ is the state space vector and control vector, respectively. The matrices, $\mathbf{Q_1}$ and $\mathbf{R}$, are the covariance weighing matrices

of $\mathbf{X}$ and $\mathbf{u}$, respectively. Then, the higher order convex function, h($\mathbf{X}$), is

$$h(\mathbf{X}) = \mathbf{X^T M_2 (X^T M_2 X) B R^{-1} B^T} \\ (\mathbf{X^T M_2 X}) \mathbf{M_2 X} \\ + (\mathbf{X^T M_2 X})(\mathbf{X^T Q_2 X}) \tag{2}$$

In this equation, $\mathbf{M_2}$ ($i = 2, .. k$) is a positive definite matrix which is an implicit function of the OPC weighting matrix, $\mathbf{Q_2}$. According to Hamiltonian optimality conditions, the control force vector is derived as

$$\mathbf{u} \\ = -\mathbf{R^{-1} B^T P X} \\ - \mathbf{R^{-1} B^T (X^T M_2 X) M_2 X} \tag{3}$$

where the first term presents the linear component of the controller which matches the control force of LQR control algorithm. The second term is the nonlinear OPC controller that presents higher order terms. The semi-positive definite matrices $\mathbf{P}$ and $\mathbf{M_2}$ are derived using stationary Riccati and Lyapunov Equations, respectively. The OPC control force is expected to yield better response mitigation for similar maximum LQR control force. In addition, nonlinear optimal control laws such as OPC are more robust than linear optimal control laws (Christofides and El-Farra, 2005). Here, the derivation of the control algorithm is based on a fully observable system, but a Kalman observer is designed to predict the entire state space vector.

3. EXPERIMENTAL SETUP

The structural model in this study is a two span bridge equipped with a semi-active MR damper attached between adjacent spans. The bridge model consists of two reinforced concrete decks, each supported by four rubber bearings. The deck in span A is 2.3 m long and has a mass of 1.48 ton, while the deck in span B is 6.0 m long and has a mass of 3.49 ton. The four supports of span A and the two left supports of span B are located on shake table A and the two right supports of span B are on shake table B, as shown in Figure 1. In cases of large difference in the

displacement responses of the spans, the gap between the spans or span and abutment will be closed and pounding occurs. Poundings will induce large acceleration spikes in the response of the spans and may cause damage to the decks.

Figure 1: The uncontrolled two span bridge model on the shake table: Left Span (A), Right Span (B)

In order to reduce the potential of pounding and its consequences, an MR damper manufactured by Sanwa Tekki from Japan is installed between span A and span B. The maximum input current for the MR Damper is 3 Amp, the force capacity is ± 30 kN, the maximum displacement is ± 70 mm, and the maximum velocity is ± 60 mm/sec. Horizontal displacements and accelerations of the spans are measured in real-time using piezoelectric sensors and accelerometers, respectively.

3.1. Hysteretic models for nonlinear bridge components

The nonlinear behavior of the bearings and the MR damper is modeled using three parallel components including a linear stiffness, damping, and hysteretic stiffness. The restoring force for the rubber bearing, F_j, and the MR damper, F_{MR}, are defined as

$$F_j = k_j \big(\alpha_j x_j + (1 - \alpha_j) z_j \big) \\ j = 1, 2 \tag{4}$$

$$F_{\mathrm{MR}} = \alpha_{\dot{x}_{\mathrm{MR}}} \dot{x}_3 + \alpha_{z_{\mathrm{MR}}} z_3 \tag{5}$$

where x_j is the linear displacement of jth rubber bearing, $\dot{x}_3$ is the velocity of the MR damper, z_j is the hysteretic displacement of jth rubber bearing, z_3 is the hysteretic displacement of the MR damper. The model parameters k_j, α_{RB}, $\alpha_{\dot{x}_{\mathrm{MR}}}$, and $\alpha_{z_{\mathrm{MR}}}$ are the

stiffness and pre-yield factor of rubber bearing, and the damping and hysteretic component of the MR damper, respectively. The subscript j takes the value of 1 for span A and 2 for span B. The hysteretic displacement follows the Bouc-Wen differential equation of the form:

$$\dot{z}_j = A\dot{x}_j - \beta|\dot{x}_j|z_j - \gamma\dot{x}_j|z_j| \qquad (6)$$
$$j = 1, 2, 3$$

The parameters $\alpha_{\dot{x}_{MR}}$ and $\alpha_{z_{MR}}$ are decomposed into passive-off and passive-on components with respect to the current, i_c, as

$$\alpha_{\dot{x}_{MR}} = \alpha_{\dot{x}_{MR_0}} + i_c\alpha_{\dot{x}_{MR_1}} \qquad (7)$$

$$\alpha_{z_{MR}} = \alpha_{z_{MR_0}} + i_c\alpha_{z_{MR_1}} \qquad (8)$$

where $\alpha_{\dot{x}_{MR_0}}$ and $\alpha_{z_{MR_0}}$ are the passive-off components and $\alpha_{\dot{x}_{MR_1}}$ and $\alpha_{z_{MR_1}}$ are the passive-on components. The model parameters of the rubber bearings are derived by fitting the experimental data of an uncontrolled bridge subjected to 70% scaled El Centro (EC70), as shown in Figure 2. As for the MR damper, data of cyclic tests with a frequency of 0.4 Hz for currents ranging between 0 and 3 Amp was provided by the manufacturing company. The corresponding calibration results are shown in Fig. 3.

3.2. Pounding Model

In the two span bridge, the Hertz Damped model (Muthukumar and DesRoches, 2006) is used to capture pounding, where the impact force, F_{impact}, is described as

$$F_{impact} = k_h(y_{12} - g_p)^r + c_h\dot{y}_{12} \qquad (9)$$

where k_h is the impact stiffness, y_{12} is the relative displacement between two adjacent nodes, g_p is the gap distance, r is the Hertz coefficient that is typically taken as 3/2, and c_h is the nonlinear damping coefficient and is computed as

$$c_h = \xi(y_{12} - g_p)^r \qquad (10)$$

where ξ is the damping constant and is calculated as follows:

$$\xi = \frac{3}{4}\frac{(1 - e^2)k_h}{\Delta v_{12}} \qquad (11)$$

where e ($= 0.6$ for concrete) and Δv_{12} are the coefficient of restitution and relative velocity before impact, respectively (Muthukumar and DesRoches, 2006). Pounding in experimental data can be detected when large spikes in the total acceleration responses are observed. For instance, acceleration spikes are observed in Figure 4 for span B of the uncontrolled bridge under KB40 but not for span A, indicating that pounding occurred between span B and the abutment.
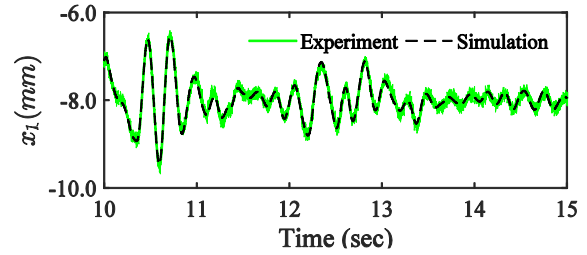

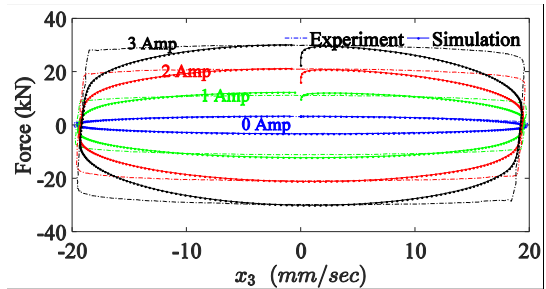*Figure 2: Time history for span A displacement (x_1).*

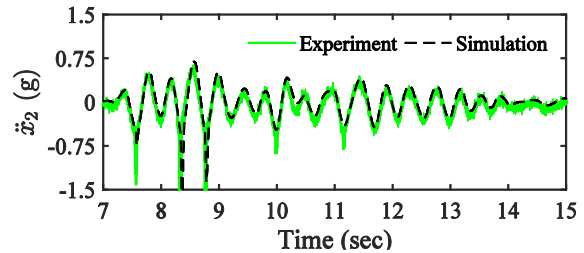*Figure 3: The MR force versus MR displacement (x_3).*

Figure 4. Time history for total acceleration of span B $(\ddot{x}_2)$.

4. IMPLEMENTATION OF SOPC

The OPC algorithm introduced in section 2 provides an active controller for a linear system with fully observable state space; however, the control problem in this study is

the semi-active control of a nonlinear system with partially observable state space. Consequently, a number of issues need to be addressed before the control system can be implemented. These issues include nonlinearity of the system, limitations associated with the semi-active control force, and partial observability of the system. Consequently, the bridge model is first linearized and the control design is implemented based on clipped optimal method (section 4.1), a second level optimization is considered to optimize the performance of the controller (section 4.2), and a Kalman based filter is designed based on the stochastically linearized system to fully predict the state space vector of the system.

4.1. Stochastic linearization

The system matrix in nonlinear hysteretic structures is not fixed, and depends on the response of the structure. Initial linear elastic properties of the system have been commonly used to present the dynamic behavior of nonlinear structures but they do not consider the intensity of external excitation in the linearization process, and may yield poor response predictions when the system is subjected to large excitations. To overcome this limitation, stochastic linearization replaces the nonlinear hysteresis component by an equivalent linear model through minimizing the residual errors arising from the linearization process (Basili and Angelis, 2007). Here, stochastic linearization is implemented for the two span bridge. The dynamic equilibrium equation of this system is presented as

$$\mathbf{M\ddot{U}} + \mathbf{C_d\dot{U}} + \mathbf{k_U U} + \mathbf{k_Z Z} = \mathbf{M\ddot{x}_g} \quad (12)$$

where the matrices, $\mathbf{M}$, $\mathbf{C_d}$, $\mathbf{k_U}$, and $\mathbf{k_Z}$ are the mass, damping, linear stiffness, and nonlinear stiffness matrices, respectively. $\mathbf{Y}$ is the linear displacement vector identified as $[x_1; \; x_2]$, and $\mathbf{Z}$ is the hysteretic displacement vector presented as $[z_1; z_2; z_3]$. The

variables x_1 and x_2 are displacements of spans A and B, and z_1, z_2, and z_3 are the hysteretic displacements of spans A and B and the MR damper, respectively. $\mathbf{\ddot{x}_g}$ is the ground motion vector applied to the two span bridge. Since Equation (6) depends only on the velocity and hysteretic displacement, the equivalent linearized equation is presented as

$$\dot{z}_j = -C_j\dot{x}_j - K_j z_j \quad (13)$$

where C_j and K_j are the linearized parameters of the velocity and hysteretic displacement, respectively. Under the assumption that $\dot{x}_j$ and z_j are zero mean joint Gaussian Processes, the linearized parameters, C_j and K_j, are obtained by partially differentiating Equation (6) with respect to $\dot{x}_j$ and z_j, respectively:

$$C_j = \frac{\partial(\dot{z}_j)}{\partial(\dot{x}_j)}, K_j = \frac{\partial(\dot{z}_j)}{\partial(z_j)} \quad (14)$$

Applying Equation (14) to Equation (6), the linearized parameters are presented as

$$C_j = \beta_j \, E\left[\frac{z \, \partial(|\dot{x}_j|)}{\partial \dot{x}_j}\right] + \gamma_j \, E[|z_j|] \quad (15)$$

$$K_j = \beta_j \, E[|\dot{x}_j|] + \gamma_j \, E\left[\frac{\dot{x}_j \, \partial(|z_j|)}{\partial z_j}\right] \quad (16)$$

Since the external excitation is assumed to be a Gaussian Process and the variables are jointly Gaussian, the linearized parameters can be evaluated in terms of the second moments as follows

$$C_j = \sqrt{2/\pi} \left[\beta_j\sigma_{z_j} + \frac{\gamma_j E(\dot{x}_j z_j)}{\sigma_{\dot{x}_j}}\right] - A_j \quad (17)$$

$$K_j = \sqrt{2/\pi)} \left[\frac{\beta_j E(\dot{x}_j z_j)}{\sigma_{z_j}} + \gamma_j\sigma_{\dot{x}_j}\right] \quad (18)$$

where $E(\dot{x}_j z_j)$ is the expected value of $\dot{x}_j z_j$, and $\sigma_{\dot{x}_j}^2$ and $\sigma_{z_j}^2$ are the variances of $\dot{x}_j$ and z_j, respectively (Socha 2008). Substituting Equation (17) and Equation (18) into Equation (12) and rearranging it in the state space, the linearized bridge model is derived as

$$\dot{\mathbf{X}} = \mathbf{A_{state}}\mathbf{X} + \mathbf{F_e}$$
$$\mathbf{X} = [\mathbf{Y}; \dot{\mathbf{Y}}; \mathbf{Z}] \qquad (19)$$

where $\mathbf{A_{state}}$ is the system matrix and $\mathbf{F_e}$ is the external excitation vector. Assuming the ground motion vector, $\ddot{\mathbf{x}}_g$, is a Gaussian process with a spectral density S_0, the system in Equation (19) can be converted into an equation for covariance, $E(\mathbf{X}\mathbf{X^T})$, in the form of:

$$\frac{d\left(E(\mathbf{X}\mathbf{X^T})\right)}{dt} = \mathbf{A_{state}}E(\mathbf{X}\mathbf{X^T})$$
$$+ E(\mathbf{X}\mathbf{X^T})\mathbf{A_{state}}^\mathbf{T} \qquad (20)$$
$$+ \mathbf{T}$$

where $\mathbf{T}$ is a vector that characterizes the ground motion as a Gaussian noise for the two span bridge, and is defined as

$$\mathbf{T} = [0; 0; 2\pi S_0; 2\pi S_0; 0; 0; 0] \qquad (21)$$

Assuming that the system is stationary, the left term in Equation (20) drops, and the covariance matrix can be derived as the solution of the Lyapunov equation:

$$0 = \mathbf{A_{state}}\mathbf{S} + \mathbf{S}\mathbf{A_{state}}^\mathbf{T} + \mathbf{T} \qquad (22)$$

where $\mathbf{S}$ is defined as the stationary covariance matrix of the state vector. Using the initial values of the linearized parameters, Equation (22) is used to compute the second moments which are then substituted in Equations (17) and (18) until the difference in the results of the successive iterations is within a prescribed error tolerance. It should be noted that the above formulation is applicable to a system that is subjected to Gaussian white noise disturbances. However, realistic ground motions are best described using filtered Gaussian processes in the frequency domain. This issue can be addressed by incorporating filters such as Modified Kanai-Tajimi filter (Xu et al., 1999; Kanai, 1957; Tajimi; 1960) in the system model of the structure such that the input to the system is white noise. Incorporating this double linear filter in the system model, a new state vector called $\mathbf{X_B}$ is defined which includes the state vector and the excitation

vector. The new modified Lyapunov equation is defined as

$$\dot{\mathbf{X}}_\mathbf{B} = \mathbf{A_B}\mathbf{X_B} + \mathbf{F_B}$$
$$\mathbf{A_B}\mathbf{S_B} + \mathbf{S_B}\mathbf{A_B}^\mathbf{T} + \mathbf{T_B} = 0 \qquad (23)$$

where $\mathbf{A_B}$, $\mathbf{S_B}$, $\mathbf{F_B}$, $\mathbf{T_B}$ are the expanded system model, covariance matrix, excitation vector, and spectral density vector, respectively.

The procedure outlined above is followed to generate a stochastic linear model of the passive-controlled system. The time-history of the displacement response of span B for the derived stochastically linearized model and fully nonlinear and the initial linear elastic models of the bridge for KB40 are shown in Figure 5. As expected, the stochastically linearized model better predicts the response of the nonlinear bridge compared to the linear elastic model.

To apply the SOPC algorithm for the semi-active control of the two span bridge model, constraints of the semi-active device must be considered. These constraints include the dependency of the applied control force on the direction of the dynamic response of the MR damper and the force capacity of the device. To incorporate these limitations in the control model, the clipped optimal strategy is applied to the derived SOPC active control force.

4.2. Second level optimization
The objective of the control strategy i.e. the relative importance of various responses of interest can be defined using the weighting matrices, $\mathbf{Q_1}$, $\mathbf{Q_2}$, and $\mathbf{R}$ in Equation (1) and (2). These weighting matrices are commonly determined based on the experience of the designer or a trial and error procedure. Such methods may not yield optimal results in most cases (Li et al., 2010). This study employs a Genetic Algorithm from Global Optimization Toolbox in MATLAB to determine optimal weighting matrices for use in computing the control force in Equation (3). For the two span bridge, one of the

primary objectives is to reduce the likelihood of pounding. Therefore, the objective function used for the second level optimization is defined as the maximum of the ratios of the maximum relative displacements in the direction of closing gap to the initial gap distance. The arguments in this optimization are the entries of the semi-positive definite matrices, $\mathbf{Q_1}$ and $\mathbf{Q_2}$. For the GA, the objective function L_2 is evaluated through a series of Monte Carlo simulations of the nonlinear bridge model subjected to stochastic realizations of the filtered Gaussian noise introduced in the previous section.
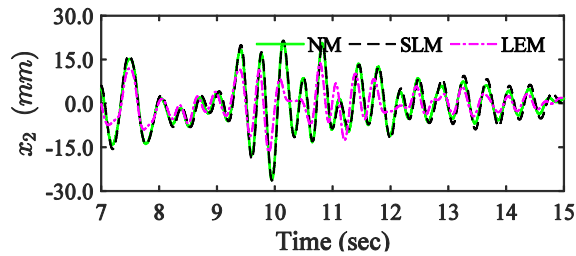

Figure 5: Displacement response of span B of Passive-Off controlled bridge. Nonlinear Model = NM; Stochastically Linearized Model = SLM; Linearly Elastic Model = LEM.

5. EXPERIMENTAL RESULTS

The performance of the proposed stochastic optimal polynomial control method in response mitigation of a nonlinear bridge equipped with a semi-active MR damper is evaluated using shake table tests. Two ground motions are selected from NGA database (Chiou et al., 2008): NGA0006 and P1046. NGA0006 was recorded during the 1940 El Centro earthquake (M_w 7.0) at the 117 El Centro Array #9 Observatory station with a distance to fault rupture of 8.3 km. The peak ground acceleration (PGA) of this ground motion is 0.45 g. P1046 was recorded during the 1995 Kobe earthquake (M_w 6.9) at the KJMA Observatory station, with a distance to fault rupture of 0.6 km. The PGA of this ground motion is 0.821 g. Kobe is a near-field earthquake characterized by high-

amplitude long period velocity pulses, large PGAs, and large permanent ground deformations. On the other hand, El Centro is a far-field earthquake that contains broadband frequency components. For shake table tests, the Kobe ground motion record is scaled by 50% (KB50), while the El Centro ground motion record is scaled by 150% (EC150).

The semi-active SOPC algorithm along with passive-off and passive-on cases are tested for the two scaled ground motions. Passive-off and passive-on cases correspond to constant input currents of zero and maximum 3 Amp, respectively. The peak of the absolute and relative displacements and total acceleration responses of bridge spans for various control cases are shown in Table 3. It is observed that the semi-active control algorithm results in reductions of x_2 and x_{12} compared to passive-off (9%, 38%) and passive on (13%, 17%), under EC150 with 45% of the current in passive-on case. The time-history of the relative displacement responses of span A and B are shown in Figure 6. Under KB50 in passive-on case, four poundings occurred between span A and abutment A and two poundings occurred between span B and abutment B. For the other two cases, i.e. passive-off bridge and the bridge equipped with the semi-active SOPC, pounding occurred once between each of the spans and their corresponding abutments.

6. CONCLUSION

In this paper, a stochastic optimal polynomial control (SOPC) method is analyzed and tested for the semi-active control of a two span bridge using shake table tests. One of the control objectives for this structure is to reduce the potential of pounding as it poses a significant problem in adjacent structures with inadequate separation gaps. In this regard, an MR damper is installed between adjacent spans to dissipate energy. The proposed clipped SOPC algorithm is

intended to optimize the performance of the MR damper compared to the two passive cases: passive-off where the input current is zero and passive-on which has the maximum input current of 3 Amp. The control design in this study considers the stochasticity of the response and excitation through a stochastic linearization. The utilized clipped optimal strategy accounts for MR damper constraints in the SOPC algorithm. Since the performance of the controller depends on the choice of the weighting matrices, a second level optimization procedure based on GA is developed to determine best entries for the weighting functions. Finally, the shake table results have shown promising results to adopt both stochastic linearization and nonlinear feedback controller in control design of nonlinear systems.

Table 3: Critical MAX response results: P-Off/On (Passive-Off/On)

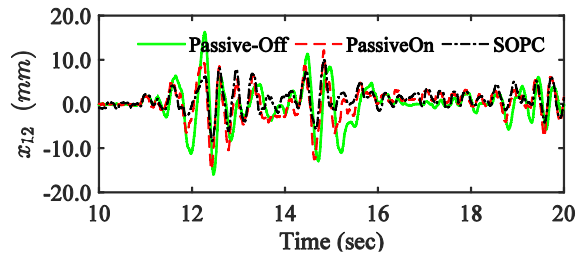| Case (EC150)	x_1 (mm)	x_2 (mm)	$\ddot{x}_1$ (g)	$\ddot{x}_2$ (g)
P-Off	7.7	22.2	0.60	0.59
P-On	10.3	23.1	0.71	1.33
SOPC	10.6	20.2	0.43	0.48
Case (KB50)	x_1 (mm)	x_2 (mm)	$\ddot{x}_1$ (g)	$\ddot{x}_2$ (g)
P-Off	25.7	39.9	0.81	1.33
P-On	28.4	40.2	1.33	1.33
SOPC	25.6	40.2	0.93	1.33

Figure 6: Experimental results for the relative displacement of the spans for bridge systems under EL150.
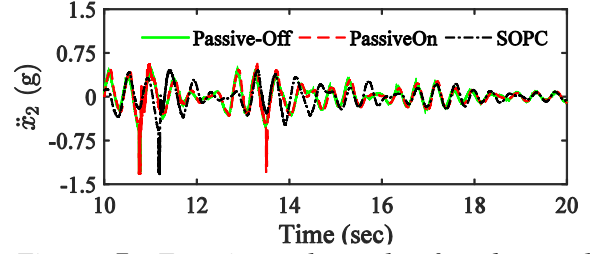

Figure 7: Experimental results for the total acceleration of span B for bridge systems under KB50.

7. REFERENCES

Agrawal, A. K., & Yang, J. N. (1996). "Optimal polynomial control of seismically excited linear structures." *Journal of engineering mechanics*, *122*(8), 753-761.

Basili, M., & De Angelis, M. (2007). "Optimal passive control of adjacent structures interconnected with nonlinear hysteretic devices." *Journal of sound and vibration*, *301*(1), 106-125.

Chiou, B., Darragh, R., Gregor, N., & Silva, W. (2008). "NGA project strong-motion database." *Earthquake Spectra*, *24*(1), 23-44.

Christofides, P. D., & El-Farra, N. (2005). "Control of nonlinear and hybrid process systems: Designs for uncertainty, constraints and time-delays." (Vol. 324). Springer.

Fan, Y. C., Loh, C. H., Yang, J. N., & Lin, P. Y. (2009). "Experimental performance evaluation of an equipment isolation using MR dampers." *Earthquake Engineering & Structural Dynamics*, *38*(3), 285-305.

Li, J., Peng, Y. B., & Chen, J. B. (2010). "A physical approach to structural stochastic optimal controls." *Probabilistic Engineering Mechanics*, *25*(1), 127-141.

Muthukumar, S., & DesRoches, R. (2006). "A Hertz contact model with non-linear damping for pounding simulation." *Earthquake engineering & structural dynamics*, *35*(7), 811-828.

Prabakar, R. S., Sujatha, C., & Narayanan, S. (2013). "Response of a quarter car model with optimal magnetorheological damper parameters." *Journal of Sound and Vibration*, *332*(9), 2191-2206.